Permeability Effects of the Ceramic Candle Filter on Back-Pulse Cleaning System

Young-Ryoul Back*, Dong-Kyu Chung*, Hyun Il Jeong**
Soo-Choon Kang*** and Myung S. Jhon******

(*Received May 21, 1996*)

The flow characteristics inside the ceramic candle filter system used in hot gas cleanup was investigated. The filter system admits high pressure back-pulse air to blow out the dust cake. The pressure drop across the filter barrier plays a critical role in dust removal. The filter medium and dust cakes were considered as multi-layered porous media and were then modeled using Darcy's effective permeability model. The k-ε model was adopted to study the turbulent flow in the filter system using FLUENT. A parametric study of the permeability of the filter media was performed to investigate the effects of dust cakes on the flow phenomena, in conjunction with the non-Darcian effect of the porous media flow and non-homogeneous boundary conditions in the inlet and the outlet.

Key Words:

Nomenclatures

C : Drag coefficient (Non-Dracian effect)
C_μ : Turbulent empirical coefficient
I : Turbulent intensity in the inlet and the outlet
k : Turbulent kinetic energy
P : Pressure
r : Radial direction in the cylindrical coordinate
S_u : Axial directional source in porous media
S_v : Radial directional source in porous media
u : Axial velocity
v : Radial velocity
x : Axial direction in the cylindrical coordinate
α : Permeability of the porous media
ε : Turbulent dissipation rate
μ : Viscosity
ρ : Density
l : Turbulent length scale

*Advanced Technology Engineering Service, Seoul, Korea.
**Power Generation Research Lab., Korea Electric Power Research Institute, Taejon, Korea
***Mechanical Engineering Dept., Carnegie Mellon University, Pittsburgh, Pennsylvania, USA
****Chemical Engineering Dept., Carnegie Mellon University, Pittsburgh, Pennsylvania, USA

1. Introduction

Integrated gasification combined cycles (IGCC) and pressurized fluidized bed combustion (PFBC) are being developed and successfully demonstrated for the next generation of electric power plants (Notestein, 1990). To achieve high overall plant efficiency, high temperature and pressure of 600~850℃ and 1.5~3.0 MPa are required to the combustion gases in order to operate the turbine system. Although the operation of filtration units prior to the turbine expansion sacrifices the internal energy of hot gases, it is necessary to insure acceptable turbine life and performance, as well as to satisfy the environmental regulations. Therefore, efficient and reliable hot gas particulate filters are the key components for the successful implementation of IGCC and other advanced power generation gas turbine cycles. Recent failure of the hot gas cleanup systems at Tidd and Kahula (AEPSC 1992,) proved the importance of hot gas cleanup technol-

ogy for the successful operation of IGCC.

Currently, advanced particle filters (APF), shown schematically in Fig. 1, are the optimal choice for the hot gas cleanup systems (cf. granular filter, candle filter, CeraMem filter(Wilson, 1989). Specifically, the candle filter is considered as one of the best candidates for the hot gas cleanup filter element. It has a hollow circular column shape with a dead end, fabricated with SiC fibers. However, as reported by the American Electric Power Service Corporation(AEPSC, 1992), after 500 hours of operation, twenty one candle elements were broken by thermal impact due to the back pulse, bridging, etc. Since the long term reliability of APF systems is a prerequisite for the success of IGCC, understanding the filtration and cleaning mechanism of the filter system is a critical issue in design and analysis. However, a stumbling block exists due to a lack of fundamental knowledge.

This paper aims to develope a simulation methodology necessary for the analysis and testing of a practical hot gas ceramic barrier filter system that satisfies the performance and operational requirements of IGCC and PFBC systems.

During the filtration operation, dust (or flyash) contained in the gases exhausted from gasifiers or combusters is sieved by filter cells, and then deposited on the surface of the ceramic filters by adhesive forces or by filling the holes in the filters by cohesive forces. In order to ensure the normal filtration operation, high pressure back-pulse air is applied to remove the dust cakes by generating the shear and normal stresses which play major roles in dust removal mechanisms. The simplified flow fields during cleaning modes are illustrated in Fig. 2. Arrows indicate the direction of flow.

Mechanical breakage of the candle filters may occur when dust fills all of the space between adjacent filters. This dust bridging may occur when the filter-cake thickness becomes larger due to non-uniform flow and deposition of dust through the filters, followed by incomplete partial removal of the filter-cakes during successive filter -cleaning back-pulses. Cracking of filters due to relief of internal stress, back-flush-induced thermal stresses, and chemical attacks (alkali) are believed to be long-term failure mechanisms.

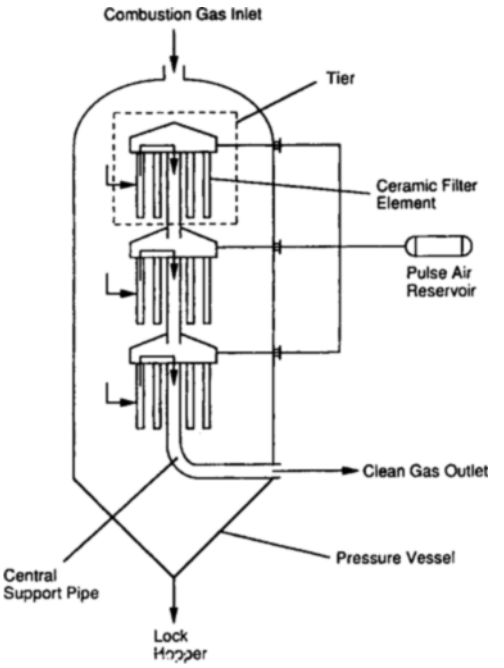

Fig. 1 Schematic of APF

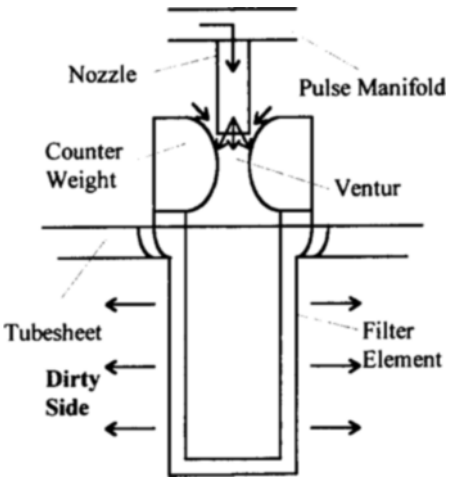

Fig. 2 Simplified view of cleaning mode

Developing the mathematical models for this complex system is a horrendous task. Therefore, in this paper we will only illustrate the mathematical modeling of filter and dust cakes and the calculation of back-pulse cleaning of a single

filter using FLUENT version 4.23 (the department of chemical engineering, Carnegie Mellon University).

2. Mathematical Modeling

The k-ε model(Hinze, 1975) was adopted to investigate the pressure drop and flow characteristics across the candle filters. The mathematical equations governing the physical phenomena in the filter are mass, momenta, turbulent kinetic energy, and turbulent dissipation rate. For the highly turbulent flow, the Reynolds stress model must be introduced to obtain a more accurate prediction. However, this requires intensive computational effort(Launder and Reece, 1975).

To investigate the flow characteristics and pressure drop across the candle filter, FLUENT (1994), based on the finite volume technique, was used to perform the numerical simulation. This software can handle various flow problems including unsteady, turbulent, radioactive and thermal flow phenomena. In addition, the chemical species transport and porous flow model are included in this code.

Figure 3 shows the cross-sectional model and physical dimensions of the candle filter the in cylindrical coordinates where x and r designate the axial and radial directions, respectively. Media 1 and media A-D represent the filter medium and the dust cakes, respectively. As shown in Fig. 3, the dust cakes are divided into 4 parts due to the fact that the permeability of the dust cake is non-homogeneous along the axial direction. The thickness of the dust cake is assumed to be 8 mm, which is also the thickness of the filter. Since the objective of this paper is to analyze back-pulse-cleaning, the pressure P_2 at the inlet is set to be higher than the pressure P_1 at the outlet. Note that the pressure difference between the inlet and the outlet is the pressure drop ($\Delta P_{12}=P_2-P_1$).

The porous media regions, which represent the dust cake and the filter medium, were mathematically modeled by Darcy's law(Darcy, 1956). In order to consider the effects of porous media, the source terms expressed in Eqs. (1) and (2) were added to the axial and the radial directional momenta equations, respectively.

$$S_u=\frac{\mu}{\alpha}u+C\frac{\rho u^2}{2} \tag{1}$$

$$S_v=\frac{\mu}{\alpha}v+C\frac{\rho v^2}{2} \tag{2}$$

where u and v are the flow velocity components in the axial and radial directions, respectively, ρ is the density of the fluid, μ is the viscosity of the fluid, α is the permeability of the porous media, and C is a drag coefficient or an inertial resistance factor. The first term accounts for the pressure drop due to permeability effects. The second terms is the inertial resistance factor which represents a non-Darcian effect (drag effect) in the porous media flow, and this contributes to the pressure gradient in the porous media by creating

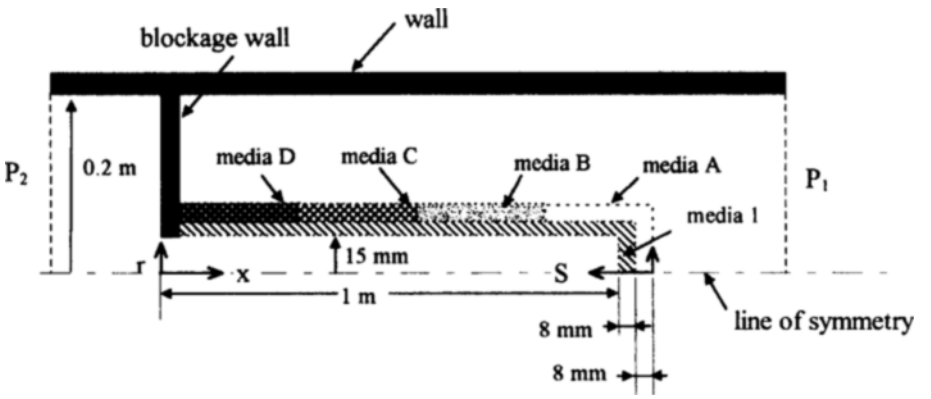

Fig. 3 Physical model for a single filter

a pressure drop that is proportional to the square of the fluid velocity.

Since the governing equations are elliptic, boundary conditions are to be prescribed on all of the boundaries. These are the inlet, outlet, wall and the line of symmetry (only half of the cross section needs to be considered, as the flow pattern is axisymmetric about the center line). Since velocity boundary conditions can not be prescribed at both the inlet and outlet boundaries, several deterministic pressure profiles and/or velocity profiles were imposed at these boundaries. Uniform pressure and non-uniform velocity (e.g. parabolic distribution profile) boundary conditions were considered. In the case of the k-ε model, the boundary conditions for the governing equations are expressed as:

$$\left.\begin{aligned} &P=P_1 \\ &\frac{\partial u}{\partial x}=\frac{\partial v}{\partial x}=\frac{\partial k}{\partial x}=\frac{\partial \varepsilon}{\partial x}=0 \end{aligned}\right] \quad \text{at } x=1.2\text{m} \tag{3}$$

$$\left.\begin{aligned} &P=P_2 \\ &I=\frac{u'}{u}=0.1 \\ &k=\frac{3}{2}(uI)^2 \\ &\varepsilon=c_\mu^{3/4}\frac{k^{3/2}}{l},\quad l=0.014\text{m} \end{aligned}\right] \quad \text{at } x=-0.2\text{m} \tag{4}$$

$$\frac{\partial u}{\partial r}=\frac{\partial v}{\partial r}=\frac{\partial k}{\partial r}=\frac{\partial \varepsilon}{\partial r}=0 \quad \text{at } r=0\text{m} \tag{5}$$

$$u=v=0 \quad \text{at } r=0.2\text{m} \tag{6}$$

where u' is the fluctuating velocity, I is the turbulent intensity, k is the turbulent kinetic energy, ε is the dissipation rate of the turbulent energy, and c_μ is an empirical constant which is set to be 0.09.

In fluid flow with porous media, the momenta equations or force balances have been established by numerous experimental observations summarized mathematically as Darcy's law. These observations were first reported by Darcy, who, based on measurement alone, discovered that the area-average fluid velocity ($\langle u\rangle$) through a porous media is proportional to the pressure difference (ΔP) established along the flow direction. Equation (7) presents the mathematical formulation of the momentum with respect to a one-dimensional forced flow

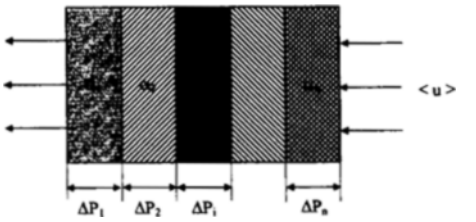

Fig. 4 One dimensional representation for Darcy's flow

$$\langle u\rangle=\alpha\Delta P \tag{7}$$

As seen in Fig. 4, when non-homogeneous porous media are arrayed in the flow direction, $\langle u\rangle$ can be expressed as follows:

$$\langle u\rangle=\alpha_1\Delta P_1=\alpha_2\Delta P_2=\cdots=\alpha_n\Delta P_n \tag{8}$$

Since the total pressure drop (ΔP_{total}) is the sum of the pressure drop at each porous medium,

$$\Delta P_{\text{total}}=\sum_{i=1}^{n}\Delta P_i=\langle u\rangle\sum_{i=1}^{n}\frac{1}{\alpha_i} \tag{9}$$

The effective permeability (α_{eff}) through all of the medium is defined as:

$$\frac{1}{\alpha_{\text{eff}}}=\frac{\Delta P_{\text{total}}}{\langle u\rangle}=\sum_{i=1}^{n}\frac{1}{\alpha_i} \tag{10}$$

By applying this effective media concept for porous media, the flow patterns and the pressure drops across the dust cake and the filter medium were analyzed.

3. Numerical Simulation

The main objective of this paper is the investigation of the flow pattern across the filter medium with several permeabilities. Before parametric studies were performed, a suitable grid system was chosen to minimize the computational effort and enhance the solution accuracy. From an investigation of grid dependence, a grid size of 90 $\times$ 50, as shown in Fig. 5, was chosen for the numerical computations. The grid points are non-uniformly distributed over the computational domain with denser clustering near the wall, inlet, outlet and porous media regions. A calculation has converged when all governing equations are balanced at each point in the interesting domain. Here, the normalized residuals for the discretized equations are on the order of $1\text{x}10^{-3}$.

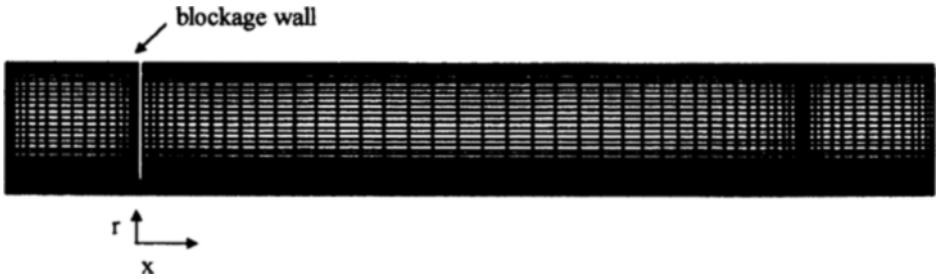

Fig. 5 Optimal grid system

There are three different turbulent models available in FLUENT: the k-ε model, the Reynolds stress model, and the Renormalization Group (RNG) model. Calculation with the k-ε model gives poor accuracy. However, this model has been widely used in engineering problems due to its simplicity and robustness. Though the prediction using the Reynolds stress model is better than that of the k-ε model, a great deal of computational effort is required and the convergence rate is slow. The RNG turbulent model shows better accuracy than the k-ε model and requires less computational effort than the Reynolds stress model. However, in this paper, we focused on the k-ε model to analyze the fluid flow because of its robustness.

3.1 Non-homogeneous boundary conditions and non-Darcian effect

To compare the effects of homogeneous pressure boundary conditions with non-homogeneous velocity boundary conditions, simulations with velocity boundary conditions whose profiles were parabolic at the inlet were performed. The axial velocity profiles at x=0.5 m, using the pressure and velocity boundary conditions, are shown in Fig. 6. Specific differences between both models are not observed in this results. Hence, the homogeneous pressure profiles are acceptable as boundary conditions in the candle filter system. In accordance with this result, the inlet boundary condition was imposed as the pressure in the present simulations and the gauge pressure in the inlet and outlet are 10^4 and 0 Pa, respectively.

Simulations were performed for two different inertial resistance factors C = 10^6 and 10^7 m^{-1}. ΔP_{12}

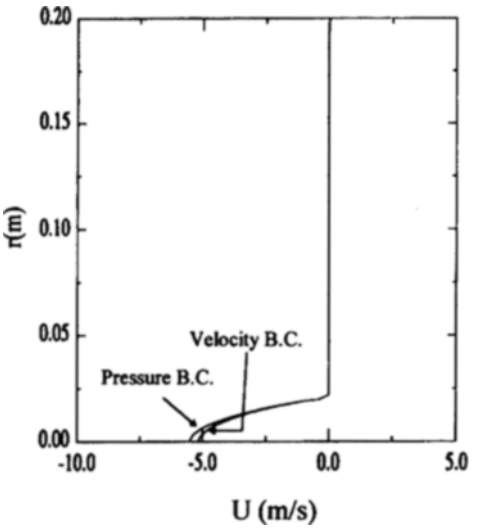

Fig. 6 The axial velocity profile at x=0.5 m for the boundary conditions

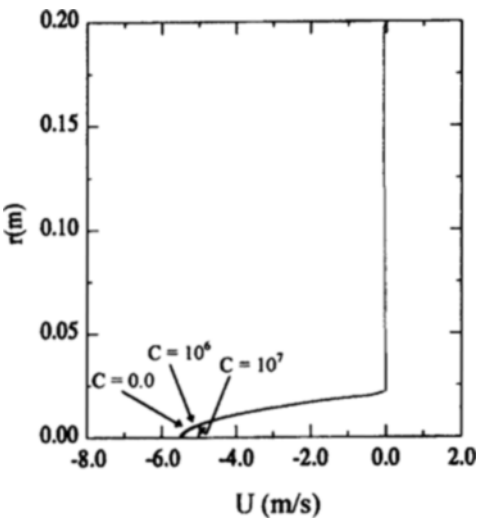

Fig. 7 The axial velocity profile x=0.5 m for the different drag coefficients

$=10^4$ Pa, $\alpha=10^{-12}$ m^2. Figure 7 shows the axial velocity profile at x=0.5 m. The flow pattern is not affected by the non-Darcian effect in the range from 0 to 10^7 m^{-1}. From this result, we found that the non-Darcian effect does not have any influence on the flow pattern inside the candle filter system. In future work, it is necessary to develop the mathematical formulation and to obtain the exact properties for the porous media, such as the candle filter, in order to enhance the simulation accuracy.

3.2 Permeability effect

A parametric study was conducted to predict the flow pattern, the pressure drop and the turbulent quantities in the candle filter with a variation of the filter permeability and turbulent model. The permeability of the filter medium is one of the critical parameters to affect the flow characteristics in the domain of interest. In Fig. 8, the distributions of streamlines for three different permeabilities, $\alpha=10^{-10}$, 10^{-11} and 10^{-12} m^2, are shown. Because the non-Darcian effect does not have any influence on the flow pattern inside the candle filter as shown in Fig. 7, we neglect the inertial resistance effect in the calculations (C=0).

The streamlines depicted in this figure show that the flow velocity is accelerated near the blockage wall. When the permeability is $\alpha=10^{-10}$ m^2, most fluids pass through the filter near the blockage wall, whereas flow through the filter neighboring the outlet does not exist. However, as decreases from 10^{-10} to 10^{-11} m^2, the flow across the filter becomes uniform. This behavior is caused by drag increasing in the porous medium according to the reduced permeability for the prescribed inertia of working fluids. A three dimensional profile of axial velocity over the entire region for $\alpha=10^{-12}$ m^2 is shown in Fig. 9. The velocity in the inner section of the filter medium is larger than that around the filter medium.

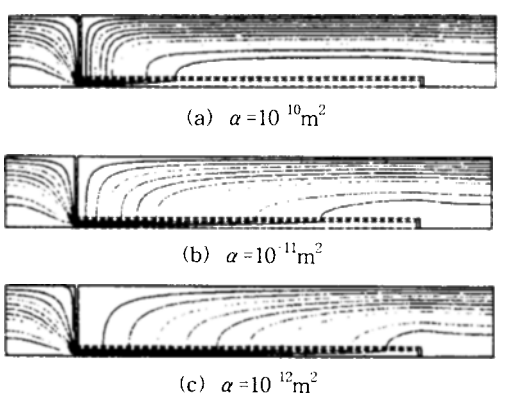

Fig. 8 Flow pattern for the three different permeabilities $\alpha=10^{-10}$, 10^{-11} and 10^{-12} m^2

Figure 10 shows the pressure drop between the inner section of the filter and the outer section of the filter along the axial direction for three different permeabilities. The pressure at the inner section of the filter maintains the inlet pressure when $\alpha=10^{-10}$ m^2, whereas the inner pressure of the

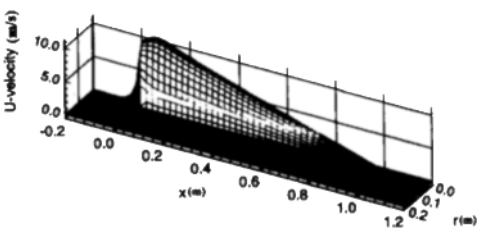

Fig. 9 Three dimensional velocity profile

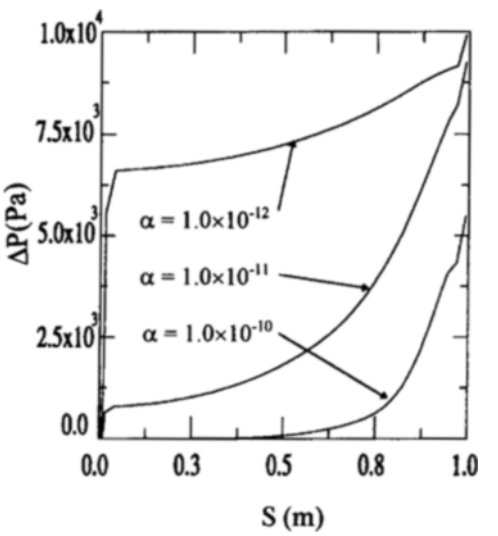

Fig. 10 The distribution of the pressure drop across the filter medium along the filter surface in the S direction for the three different permeabilities shown in Table 1.

Table 1 The permeabilities of the filter medium and the dust cake.

Case #	α_1 (m^2)	α_A (m^2)	α_B (m^2)	α_C (m^2)	α_D (m^2)	α_{eff} (m^2)
Case 1	10^{-12}	1.00×10^{-11}	1.00×10^{-11}	1.00×10^{-11}	1.00×10^{-11}	9.09×10^{-13}
Case 2	10^{-12}	1.50×10^{-11}	1.50×10^{-11}	5.00×10^{-12}	1.50×10^{-12}	9.09×10^{-13}
Case 3	10^{-12}	2.25×10^{-12}	7.50×10^{-12}	7.50×10^{-12}	2.50×10^{-12}	9.09×10^{-13}
Case 4	9.09×10^{-13}	9.09×10^{-13}	9.09×10^{-13}	9.09×10^{-13}	9.09×10^{-13}	9.09×10^{-13}

filter for $\alpha=10^{-10}$ and 10^{-11} m^2 suddenly drops to the outlet pressure after the fluid passes the blockage wall. This phenomenon occurs because most fluids are discharged through the filter near the blockage wall in the case of $\alpha=10^{-10}$ and $10^{-11}m^2$, but the flow when $\alpha=10^{-12}$ m^2 is uniform over the entire filter surface. The three dimensional pressure profile for $\alpha=10^{-12}$ m^2 is shown in Fig. 11 to visualize the pressure drop across the filter medium when the fluid passes through the filter.

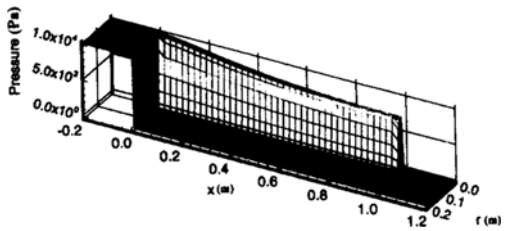

Fig. 11 Three dimensional pressure profile

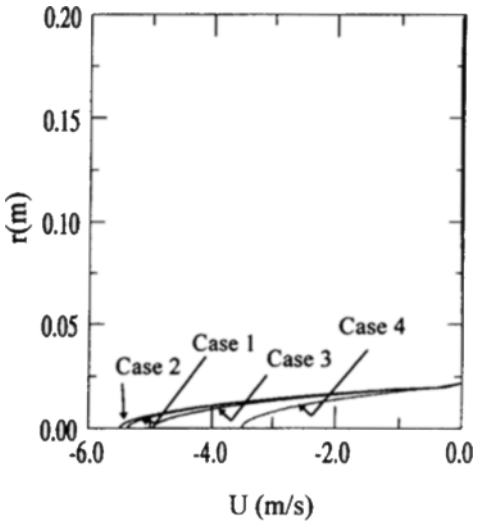

Fig. 12 The axial velocity profile x=0.5 m for the three different permeabilities

3.3 Effective porous media

To investigate the effective porous media concept, simulations for four cases were performed. The permeabilities for the filter media and the dust cakes are shown in Table 1, and the effective permeability, α_{eff}, is constant for all cases. Case 4 represents a homogeneous porous media combined with a filter medium and a dust cake.

Figure 12 shows the axial velocity profile at x= 0.5 m for four different permeabilities. The velocity profiles for the four cases are quantitatively similar except near the line of symmetry. Because of the complexity of turbulence and its dependence on the permeability of the porous media, it is difficult to explain the specific discrepancy between cases 1 and 4 for the different predicted axial velocities. Therefore, further study is necessary to verify the effective medium theory.

4. Conclusions

In order to simulate the aerodynamics in the back-pulse cleaning of a single ceramic filter, FLUENT version 4.23 was used. Results from the k-ε models were obtained for several physical parameters by performing the numerical simulation at an optimal grid size of 90×50, which was obtained from testing and comparing several different grid sizes. Some important physical aspects for the flow pattern and pressure distribution were also investigated by the numerical analysis.

As the filter permeability, α, decreases from 10^{-10} to 10^{-12} m^2, the mass flow rate through the candle filter decreases noticeably as well. The non-Darcian effect can be ignored in the flow pattern inside the candle filter system. The homogeneous pressure profiles can be used as boundary condi-

tions successfully. The effective permeability theory is easy to apply but, in order to analyze the candle filter application, more rigorous effective permeability theories are required.

It is recommended that numerical simulations for the unsteady state problem should be attempted in order to yield more accurate results for the aerodynamics of back-pulse cleaning systems. To predict the flow patterns and the pressure drop across the filter medium and the dust cake accurately, further studies are required.

References

American Electric Power Service Corporation: 1992, PFBC HGCU Test Facility Technical Progress Report, Fourth Quarter, CY1992, Columbus, Ohio.

Darcy, H., 1956, *Les Fontains Publiques de la ville de Dijon*, Victor Damont, Paris.

FLUENT's Manual, 1994, Vol. 1~5, Lebanon, NH 03766.

Hinze, J. O., 1975, *Turbulence* : McGraw-Hill Publishing Co., New York, N.Y.

Launder, B. E. and Reece, G. J., 1975, "Progress in the Development of a Reynolds-Stress Turbulence Closure," *J. Fluid Mech.*, 68 (3), p. 537.

Notestein, J. E., 1990, Commercial Gasifier for IGCC Application Study Report, *DOE/METC-91/6118*.

Wilson, K. B., 1989, "Performance Evaluation of a Screenless(Counter-Current) Granular Bed Filter on a Subpilot-Scale PFBC," *Proc. of the 6th Annual Coal-Fueled Heat Engine and Gas Stream Cleanup Systems Contractors Review Meeting*, *DOE/METC-89/6101*, pp. 293~303.